

# Isolation and Characterization of Biodegradable Chitosan Films from Black Soldier Fly Spent Pupal Shells for Food Packaging Applications

Zarul Ikmal Zainol Abidin<sup>1</sup>, Nor Hidawati Elias<sup>1,2\*</sup>, Nurhadijah Zainalabidin<sup>3</sup>

<sup>1</sup>Faculty of Chemical Engineering & Technology, Universiti Malaysia Perlis (UniMAP), 02600 Arau, Perlis, Malaysia

<sup>2</sup>Centre of Excellence for Biomass Utilization, Universiti Malaysia Perlis (UniMAP), Perlis, Malaysia

<sup>3</sup>Faculty of Mechanical Engineering & Technology, Universiti Malaysia Perlis (UniMAP), 02600 Arau, Perlis, Malaysia

## ABSTRACT

*In response to increasing global demand for sustainable packaging alternatives, this study investigates the feasibility of producing biodegradable chitosan films from Black Soldier Fly (BSF) spent pupal shells for food packaging applications. The purpose of this study is to extract chitin from BSF spent pupal waste, convert it into chitosan films for physicochemical, mechanical, and structural characterization. Chitin was isolated through sequential demineralization, deproteinization, and decolourization, followed by chemical deacetylation to produce chitosan with a high yield ( $53.48 \pm 1.46\%$ ) and degree of deacetylation ( $92.69 \pm 0.44\%$ ). The resulting BSF-based chitosan films were evaluated for solubility, moisture content, water vapor permeability, tensile strength, elongation at break, and Young's modulus. While BSF-chitosan films demonstrated good solubility and has moderate barrier properties, it has lower mechanical strength than commercial chitosan films. Through the comparative analysis, the BSF-based films are the thinnest ( $0.063 \pm 0.010$  mm), opaquest ( $3.432 \pm 0.018\%$ ), highly soluble ( $42.4 \pm 1.47\%$ ), has modest moisture content ( $4.88 \pm 4.58\%$ ) and low water permeability properties ( $0.24 \pm 0.23 (\times 10^{-10} \text{ g/Pa}\cdot\text{s}\cdot\text{m})$ ). However, blending BSF and commercial chitosan significantly enhanced tensile properties and film uniformity. FTIR and XRD analyses confirmed characteristic functional groups and crystalline structures suitable for packaging applications. The presence of multiple functional groups (hydroxyl, amine, and alcohol) and a high crystallinity index ( $\geq 85\%$ ) are expected to enhance the films' barrier performance and mechanical strength. These findings highlight the potential of BSF spent pupal shell-based chitosan as a sustainable and effective material for biodegradable food packaging, offering a viable alternative to conventional plastics and contributing to reduce plastic pollution.*

**Keywords:** BSF Spent Pupal Shell, Biopolymer, Chitin, Chitosan Film, Food packaging

## 1. INTRODUCTION

Increasing global demand for sustainable and environmentally friendly packaging solutions has catalysed substantial research into biodegradable alternatives, marking a significant shift from conventional synthetic plastics. In this context, chitosan films derived from insect sources, particularly the chitin-rich spent pupal shell or cocoon of insects such as the black soldier fly (BSF), have emerged as a promising avenue (Pedrazzani et al., 2024). Chitosan, a polysaccharide derived from chitin through deacetylation, offers a compelling array of properties that render it well-suited for diverse applications in food packaging. These include biocompatibility, biodegradability, and antimicrobial activity (El Knidri et al., 2018), making it a viable candidate to replace traditional petroleum-based plastics that contribute significantly to environmental pollution and resource depletion (Ssekatawa et al., 2021).

\*Corresponding author: [norhidawati@unimap.edu.my](mailto:norhidawati@unimap.edu.my)

Unlike crustacean shell wastes, which are subject to logistical challenges and seasonal availability, insects like the BSF present a sustainable year-round source of chitin. The BSF has garnered attention for its efficient conversion of organic waste into biomass, including its chitin-rich spent pupal shell (Hahn et al., 2020). This waste stream, often overlooked, holds significant potential for valorisation into valuable biomaterials such as chitosan. By harnessing BSF pupal shell waste for chitosan production, researchers can mitigate environmental impacts associated with traditional waste disposal while simultaneously addressing the growing demand for eco-friendly packaging solutions (Gera et al., 2023). Nevertheless, there is a lack of understanding regarding the potential of developed insect chitosan films in terms of the effect of parameters and their characterization. These aspects are important for the food packaging industry to ensure the safety and extended lifespan of packaged foods and to reduce plastic pollution in an environmentally friendly way. Therefore, the objective of this study is to investigate the potential of BSF spent pupal shell to be produced as chitosan films. Also, this study aims to investigate the physicochemical, mechanical properties and microstructural analysis of chitosan composite films. Techniques such as FTIR, and X-ray diffraction provided insights into the structural features, crystalline properties, and performance of the films. A comprehensive understanding of these properties is crucial for optimizing film fabrication processes and tailoring them to the specific demands of food packaging applications, thereby advancing the development of insect-derived biopolymers as sustainable alternatives to conventional petroleum-based plastics.

## **2. MATERIALS AND METHODS**

### **2.1 Raw Materials and Chemicals**

The BSF spent pupal shell were collected from a local supplier, Unique Biotech Sdn Bhd located in Sepang, Selangor, Malaysia. Chemicals i.e. hydrochloric acid (HCl), sodium hydroxide (NaOH), potassium permanganate (KMnO<sub>4</sub>), oxalic acid (C<sub>2</sub>H<sub>2</sub>O<sub>4</sub>), acetic acid (CH<sub>3</sub>COOH), glycerol (C<sub>3</sub>H<sub>8</sub>O<sub>3</sub>), sodium chloride (NaCl) and standard chitosan were purchased from Sigma-Aldrich (Merck, Darmstadt, Germany). All the chemicals used were of analytical grades with at least 98% purity unless stated otherwise.

### **2.2 Chitosan Extraction from BSF Spent Pupal Shell**

#### **2.2.1 BSF Spent Pupal Shell Pretreatment and Powder Preparation**

Prior to the process of chitin isolation, 100 g of BSF spent pupal shell were pre-treated through multiple steps of cleaning and drying in an oven at 60°C overnight to remove impurities and dust. Then, dried BSF spent pupal shell sample were ground to increase the accessibility of the chemicals to chitin and chitosan (Hahn et al., 2020). The dried BSF spent pupal shells were ground and sieved into 150 µm size of powder particles that are suitable for chitin isolation. The BSF spent pupal shell powder was kept in an airtight plastic bag for further use (Saenz-Mendoza et al., 2020).

#### **2.2.2 Chitin Isolation**

In this work, a multi-step chemical processes namely: demineralization, deproteinization and decolourization, were adapted to isolate chitin from BSF pupal shells (Mohan et al., 2020). Firstly, for demineralization, 5 g of BSF spent pupal shell powder was demineralized with 100 ml of 2 M HCl at 80°C for an hour in a 250 ml flask. The demineralized sample was filtered and rinsed with distilled water to remove the solubilized salts from the chitin (Saenz-Mendoza et al., 2020). Then, deproteinization was performed using 100 ml of 1 M NaOH onto the insect sample at 80°C for an hour. Washed deproteinized sample were decolorized by adding 100 ml of 1% (w/v) KMnO<sub>4</sub> solution into sample and heated at 80°C. After 20 mins of reaction, 100 ml of 1% (w/v) C<sub>2</sub>H<sub>2</sub>O<sub>4</sub> was added and heated (80°C) for another an hour. A white-grey final product (BSF chitin) was

then washed through a cloth strainer using distilled water and dried in the oven at 60°C, 24 hours for further application in chitin deacetylation. Yield of chitin was calculated based on the dry weight through gravimetric analysis, measuring the weight of raw material ( $A_1$ ) and the weight of isolated chitin ( $A_2$ ) according to the following Eq. (1) (Khatami et al., 2024):

$$\text{Chitin yield (\%)} = \frac{A_2}{A_1} \times 100 \quad (1)$$

### 2.2.3 Deacetylation of Chitin to Chitosan

Fifty ml of 50% (w/v) NaOH solution was added to a 10 g of isolated chitin sample and placed in a 250 ml flask. The sample solution was heated (120°C) and continuously stirred for 2 hours. Upon completion, the solution was filtered and repeatedly rinsed with distilled water until a state of neutrality is reached. The deacetylated chitosan (solid phase) was then dried (60°C) for 24 hours. A set of analyses, including yield and degree of deacetylation of chitosan was carried out for estimation of the quantitative data of the chitosan using various analytical methods. The chitosan yield was calculated based on the dry weight through gravimetric analysis, measuring the weight of isolated chitin ( $A_2$ ), and the weight of acetylated chitosan ( $A_3$ ) based on the following Eq. (2):

$$\text{Chitosan yield (\%)} = \frac{A_3}{A_2} \times 100 \quad (2)$$

To determine the degree of deacetylation (DD) chitin to chitosan, 0.1 g of chitosan was mixed with 10 ml of 0.3 M HCl solution and distilled water to form a volume of 50 ml. The titration process was performed with 50 ml of 0.3 M NaOH solution using a few drops of methyl red that acted as a pH indicator. The deacetylation rate was calculated using the Eq. (3):

$$DD(\%) = \frac{\phi}{\frac{W \times 161 \times \phi}{204} + \phi} \times 100 \quad (3)$$

and,

$$\phi = \frac{N_A V_A \times N_B V_B}{1000}$$

where  $\phi$  is the number of mole of HCl reacted in mole,  $N_A$  is the concentration of HCl in mol/L,  $N_B$  is the concentration of NaOH in mol/L,  $V_A$  is the volume of HCl in ml,  $V_B$  is the consumed volume of NaOH in ml and  $W$  is the weight of chitosan in g.

### 2.3 BSF-based Chitosan Film Preparation

A chitosan film forming solution was prepared by dissolving 1% (w/w) BSF-based chitosan into 1% (v/v)  $\text{CH}_3\text{COOH}$  solution at 27°C under continuous stirring for 24 hours. Then, 30% (w/w) of glycerol was added and stirred (30 mins) until the solution was homogenised. The chitosan-film solution was then centrifuged (5000 rpm, 25°C) for 10 minutes to separate the impurities. Then, 10 ml of chitosan-film supernatant was immediately poured onto petri dish and allowed to dry in an oven (80°C) for 24 hours. A solid product (BSF-chitosan film) was formed and set for further analysis. A chitosan-film from commercial chitosan was also prepared as a control.

## 2.4 Mechanical Properties Analysis

The mechanical properties of chitosan film was measured using a Universal Testing Machine with a 50 N load cell. Each film was cut into 7 cm × 2 cm rectangular samples, and maintained the conditions of a distance of 3 cm between the clamping pincers and the speed of 10 mm/min deformation (Bhuvaneshwari et al., 2011). The tensile strength, elongation at break, and Young's modulus was calculated from the slope between the x and y strain, maximum strength, and maximum strain, respectively, or using three equations, which are Eq. (4), Eq. (5) and Eq. (6) to determine the tensile strength ( $\sigma$ ), elongation at break and Young's modulus, respectively.

$$\sigma \text{ (MPa)} = \frac{F}{A} \quad (4)$$

$$\text{Elongation at break (\%)} = \frac{L}{L_0} \times 100 \quad (5)$$

$$E = \frac{\sigma}{\varepsilon}, \varepsilon = \frac{\Delta L}{L_0} \quad (6)$$

where  $F$  is the maximum applied force at break (N),  $A$  is the film's cross-sectional area (m<sup>2</sup>),  $L$  is the elongation of film at break (mm),  $L_0$  is the initial distance between clamps,  $\varepsilon$  is the stress at break (MPa) and  $\Delta L$  is the change in distance (mm) (Liu et al., 2020; Rachtanapun et al., 2021; Saenz-Mendoza et al., 2020; Yan et al., 2023).

## 2.5 Physical Properties of Chitosan Films

### 2.5.1 Thickness

Film thickness was analysed using a digital micrometre, with an accuracy of  $\pm 0.001$  mm, measuring at three different random positions of each film sample for precise data.

### 2.5.2 Color and Opacity

Colour analysis was carried out using a calorimeter by placing a film on a white calibration plate for the measurements at three random positions on the surface. The CIELAB ( $L^*$ ,  $a^*$ ,  $b^*$ ) scale was used to determine the colour parameters; therefore, both equation, that included, hue angle ( $^\circ$ h) value,  $\tan^{-1}(b^*/a^*)$  and chroma ( $C^*$ ),  $(a^{*2} + b^{*2})$ , was used to calculate the whiteness index ( $WI$ ) by using Eq. (7) and the total colour difference ( $\Delta E^*$ ) by using Eq. (8) (Saenz-Mendoza et al., 2020):

$$WI = 100 - \sqrt{(100 - L^*)^2 + a^{*2} + b^{*2}} \quad (7)$$

$$\Delta E^* = \sqrt{(L_1^* - L_2^*)^2 + (a_1^* - a_2^*)^2 + (b_1^* - b_2^*)^2} \quad (8)$$

Film opacity was analysed using a UV-Vis light spectrophotometer. A rectangular film (4 cm × 1 cm) was positioned in a spectrophotometer cell. The film absorbance was tested at 600 nm. The opacity of the film was calculated using Eq. (9). Three replications of the experiment are notable for a precise mean data of the film opacity (Sutharsan et al. 2022).

$$\text{Opacity (\%)} = \frac{\text{Absorbance } A_{600nm}}{\text{Thickness, } x} \quad (9)$$

### 2.5.3 Solubility

The film solubility was assessed by placing a rectangular film (1 cm × 1 cm) inside a desiccator for 7 days; then, the sample was weighed, and 80 ml of distilled water was added at room temperature (20 ± 5°C) and continuously stirred for an hour. After that, the sample was filtered through a filter paper and dried in an oven at 60°C. The solubility of chitosan film was verified using Eq. (10):

$$\text{Solubility (\%)} = \frac{(\text{Initial dry weight} - \text{Final dry weight})}{\text{Initial dry weight}} \times 100 \quad (10)$$

### 2.5.4 Moisture Content

A 1 cm × 1 cm film sample was dried in an oven at 105 °C overnight until a constant weight was achieved. Moisture content was determined based on the average of three replicates. The moisture content was then calculated using Eq. (11):

$$\text{Moisture content (\%)} = \frac{\text{Initial weight} - \text{Final weight}}{\text{Initial weight}} \times 100 \quad (11)$$

### 2.5.5 Water Permeability Properties

The film was placed on a test cell containing a desiccant material that was used to generate relative humidity. Then the cell was placed inside a desiccator containing a saturated sodium chloride (NaCl) solution. The process was carried out at room temperature for 7 hours. The weight change of the cell was quantified each hour. The slope resulting from the weight change to time was calculated by the linear regression method (Suenz-Mendoza, et al., 2020). The transmission rate of water vapour (*WVTR*) was determined from the slope of a straight line divided by the permeation area of 0.0031 m<sup>2</sup>. Therefore, water vapour permeability (*WVP*) was calculated using Eq. (12), where *x* is the film thickness (m) and  $\Delta P$  is the water vapour partial pressure difference between two sides of the film (1730 Pa):

$$WVP (g/Pa \cdot s \cdot m) = WVTR \left( \frac{x}{\Delta P} \right) \quad (12)$$

## 2.6 Structural Analysis of Chitosan Films

### 2.6.1 X-ray Diffraction

X-ray patterns of the chitosan film were investigated using an X-ray diffractometer (Bruker, United States) equipped with a detector and a radiator. The conditions of the experiment were 40 kV, current of 30 mA, diffraction angle of 5° to 40° and a scanning speed of 1 min<sup>-1</sup> (Khatami et al., 2024). The average of triplicate diffraction data was recorded from 2θ (angle of incidence of the X-ray beam on the film) values. The crystallinity index (CrI) of the film was determined using Eq. (13), where *A<sub>c</sub>* is the area of the crystalline region and *A<sub>a</sub>* is the area of the amorphous region.

$$CrI = \left( \frac{A_c}{A_c + A_a} \right) \times 100 \quad (13)$$

### 2.6.2 Fourier-transform Infrared Spectroscopy

To determine the presence of functional group in BSF-chitosan film, the analysis was done through a FTIR (Perkin Elmer Spectrum-65, United States) with the following conditions: resolution of  $4\text{ cm}^{-1}$ , wavenumber ( $1/\lambda$ ) ranges from  $450$  to  $4000\text{ cm}^{-1}$ , with a total of 32 scans per sample (Yan et al., 2023).

### 2.7 Statistical Analysis

The experiments were run in triplicate. The data was expressed as mean  $\pm$  standard deviation. The comparisons of mean between groups of samples was performed by one-way analysis of variance (ANOVA) and was considered significant if  $p \leq 0.05$ .

## 3. RESULTS AND DISCUSSION

### 3.1 Determination of Chitin and Chitosan Yields and Degree of Deacetylation

Table 1 depicts the extraction of chitin and chitosan from Black Soldier Fly (BSF) spent pupal shells which yielded  $10.39 \pm 4.15\%$  chitin and  $53.48 \pm 1.46\%$  chitosan, with a high degree of deacetylation (DD) of  $92.69 \pm 0.44\%$ .

**Table 1:** Yields and Degree of Deacetylation (DD) of Chitin and Chitosan


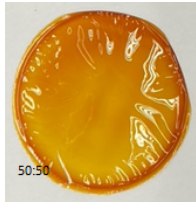

BSF Chitin & Chitosan	Yield (%)	Degree of Deacetylation (DD) (%)
Extracted Chitin	$10.39 \pm 4.15$	-
Deacetylated Chitosan	$53.48 \pm 1.46$	$92.69 \pm 0.44$

These results indicate an efficient deacetylation process, producing high-quality chitosan suitable for various applications. Comparatively, Lagat et al. (2021) reported chitin yields of 10.18% and 11.85% using chemical and biological extraction methods, respectively. They also obtained a maximum chitosan yield of 6.58% via chemical treatment, with a lower DD of 18.52% and 37.38% for pupae and adults, respectively. Soetemans et al. (2024), obtained chitin yields ranging from 8% to 24% from various BSF life stages, with shedding and cocoons being most rich in chitin. The chitosan yield, on the other hand, is comparable to the  $64.22 \pm 0.79\%$  yield reported by Yuan et al. (2024) under optimized chemical extraction conditions. These differences in yield can be attributed to various factors such as the deproteinization and demineralization efficiency, the stage of insect development, and the specific strain or diet of BSF used. The DD obtained in this study is slightly lower than the 89% reported by Soetemans et al. (2024) for chitosan derived from BSF chitin after 3 hours of deacetylation, but still within the acceptable range for effective chitosan functionality. The higher chitosan yield and DD in the current study suggest improved extraction and deacetylation processes, enhancing the potential for industrial applications of BSF-derived chitosan.

### 3.2 Physical Properties of Chitosan Films

Table 2 shows the physical properties of chitosan films derived from BSF spent pupal shells compared with the films made from a 50:50 BSF-commercial chitosan blend and pure commercial chitosan. The BSF chitosan film exhibited the greatest thickness ( $0.063 \pm 0.01\text{ mm}$ ), followed by the commercial chitosan ( $0.093 \pm 0.01\text{ mm}$ ) and the blended film ( $0.040 \pm 0.22\text{ mm}$ ). This suggests that chitosan derived solely from BSF tends to form a denser film matrix. The BSF chitosan film also showed the highest solubility ( $42.4 \pm 1.47\%$ ) compared to the blended ( $31.10 \pm 2.59\%$ ) and commercial chitosan films ( $37.8 \pm 6.13\%$ ). Moisture content among the films

**Table 2:** Physical Properties of Chitosan Films

Physical Properties	BSF chitosan (100%)	BSF chitosan: Commercial chitosan (50:50)	Commercial chitosan (Control)
Thickness (mm)	0.063 ± 0.01	0.040 ± 0.22	0.093 ± 0.01
Solubility (%)	42.4 ± 1.47	31.10 ± 2.59	37.8 ± 6.13
Moisture Content (%)	4.88 ± 4.58	4.3 ± 0.99	4.18 ± 1.887
WVP (×10 <sup>-10</sup> g/Pa·s·m)	0.24 ± 0.43	1.96 ± 4.1	0.17 ± 1.0
Opacity (%)	3.432 ± 0.02	2.117 ± 0.18	1.846 ± 0.01
Whiteness Index, <i>WI</i>	17.25 ± 1.43	35.23 ± 2.92	42.28 ± 2.13
Color Characteristic:			
<i>L</i> <sup>*</sup>	27.54 ± 1.97	44.23 ± 2.52	50.56 ± 3.37
<i>a</i> <sup>*</sup>	27.76 ± 0.448	19.26 ± 0.338	15.60 ± 0.173
<i>b</i> <sup>*</sup>	28.71 ± 0.94	26.68 ± 2.14	25.25 ± 1.75
Quality of film			

showed no significant difference, ranging from 4.18% to 4.88%. However, the water vapor permeability (WVP) was highest in the blended film ( $1.96 \times 10^{-10}$  g/Pa·s·m), followed by BSF chitosan ( $0.24 \times 10^{-10}$  g/Pa·s·m), and lowest in the commercial chitosan film ( $0.17 \times 10^{-10}$  g/Pa·s·m). The increase in WVP in the blended film may be due to structural rearrangement during mixing, leading to a more porous matrix, as discussed by No et al. (2007).

The colour of packaging films influences the appearance and consumer acceptance of the product (Sutharsan et al., 2022). In terms of opacity, the pure chitosan film (control) had the opacity of  $1.846 \pm 0.01\%$ . BSF chitosan also recorded the highest value ( $3.432 \pm 0.02\%$ ), which may be attributed to the presence of natural pigments and the degree of acetylation. The colour analysis results showed no significant difference of variables between standard chitosan films, even though the whiteness index ranges from around 17 to 42. Conversely, the *a*<sup>\*</sup> value provided a better indication of the film colour, as the insect-based chitosan films exhibited a greater tendency toward red compared to the standard films, indicating a shift toward a yellowish tonality. Therefore, the full proportion of insect chitosan film had the highest chroma value, and thus resulted in the lowest whiteness index and greatest total colour difference with the standard chitosan films. Additionally, the colouration of insect chitosan films could be due to presence of unremoved colour pigments during chitin treatment. The film quality also varied visually, with BSF chitosan films appearing more brittle and irregular, while the commercial and blended films were smoother and more uniform. Overall, while BSF chitosan demonstrates promising film-forming capabilities, blending with commercial chitosan may improve its mechanical and barrier properties.

### 3.3 Mechanical Properties of Chitosan Films

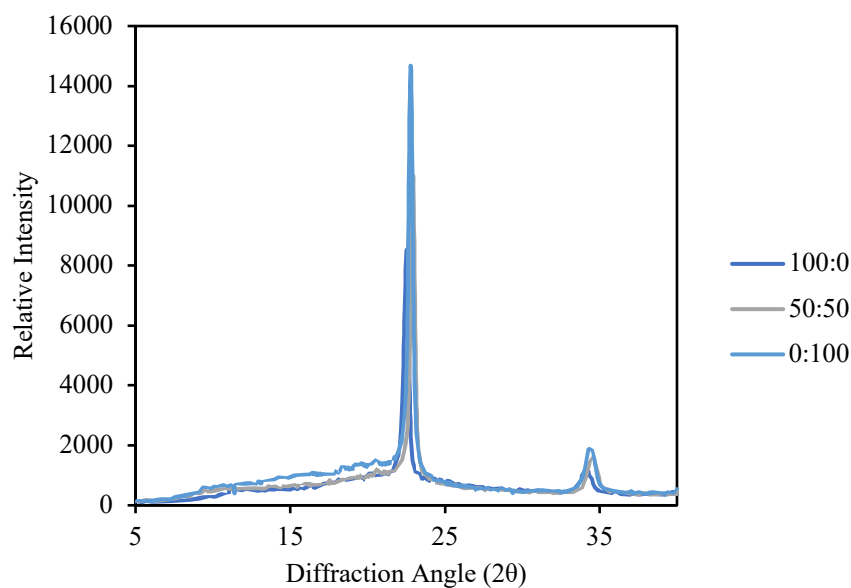
Table 3 shows the mechanical properties of the chitosan films where notable variation depending on the chitosan composition was observed. The commercial chitosan film exhibited the highest tensile strength ( $44.5 \pm 6.9$  MPa), break elongation ( $35.6 \pm 5.5\%$ ), and Young's modulus ( $519.5 \pm 2.5$  MPa), indicating superior mechanical integrity and flexibility. In comparison, the film made from 100% BSF chitosan demonstrated significantly lower mechanical performance, with a tensile strength of  $28.7 \pm 6.1$  MPa, break elongation of  $17.8 \pm 4.7\%$ , and Young's modulus of  $316.5 \pm 1.2$  MPa. Interestingly, the 50:50 blend of BSF and commercial chitosan showed intermediate properties, with a marked improvement over pure BSF chitosan tensile strength of  $39.9 \pm 1.8$  MPa, break elongation of  $24 \pm 2.3\%$ , and Young's modulus of  $463.7 \pm 4.8$  MPa. These results suggest that blending BSF-chitosan with commercial chitosan enhances the mechanical properties of the film, likely due to better polymer network formation and compatibility, making the blended film a promising alternative material with improved strength and flexibility compared to BSF chitosan alone.

**Table 3:** Mechanical Properties of Chitosan Films

Mechanical Properties	BSF chitosan (100%)	BSF chitosan: Commercial chitosan (50:50)	Commercial chitosan (Control)
Tensile Strength (MPa)	$28.7 \pm 6.1$	$39.9 \pm 1.8$	$44.5 \pm 6.9$
Break Elongation (%)	$17.8 \pm 4.7$	$24 \pm 2.3$	$35.6 \pm 5.5$
Young's Modulus (MPa)	$316.5 \pm 1.2$	$463.7 \pm 4.8$	$519.5 \pm 2.5$

### 3.4 Structural Properties of Chitosan Films

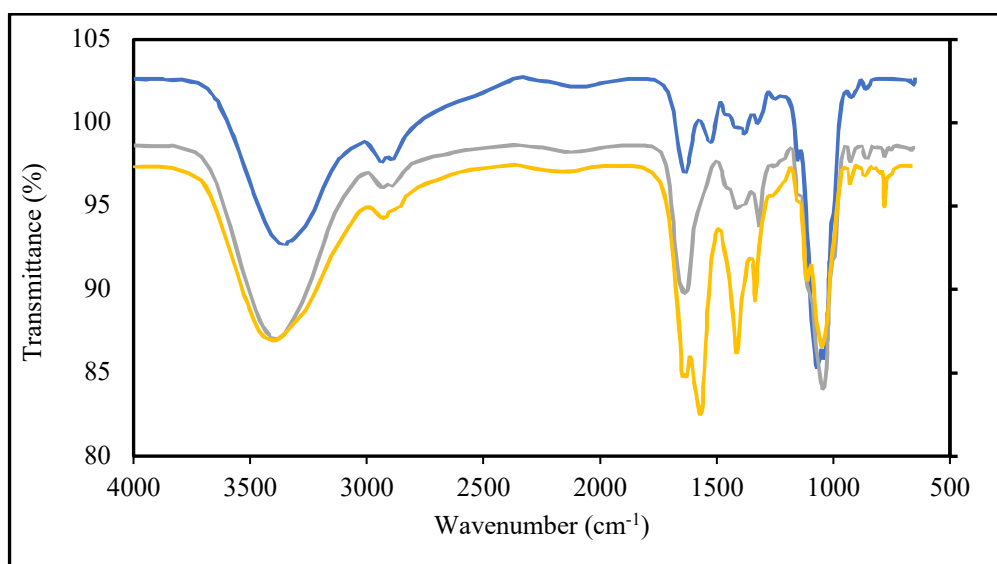
Figure 1 shows an X-ray diffraction pattern of chitosan films, with two peaks of larger intensity around  $2\theta \approx 23.3^\circ$  and  $34.7^\circ$ , and three peaks of less intensity around  $2\theta \approx 9.5^\circ$ ,  $17.1^\circ$  and  $20.4^\circ$ . Among the large peak intensities, the sharp, distinct and long-range order peaks along  $2\theta \approx 23.3^\circ$  corresponded to the well-ordered crystalline structure of films, and the broad peaks across  $2\theta \approx 34.7^\circ$  indicated the presence of random arrangement amorphous structure (Hanh et al., 2020; Mohan et al., 2020).



**Figure 1:** Infrared Spectra of Chitosan Films.



Figure 2 shows the infrared spectra of both standard and insect chitosan films. Although the films were varied by formulations, the patterns of each spectrum were similar to each other in between ranges of wavenumbers. All the films had O-H stretching in the range of  $3356.29\text{ cm}^{-1}$  to  $3400.37\text{ cm}^{-1}$ , indicating the presence of carboxylic acid corresponded to acetic acid. Meanwhile, the films had sharp peaks of H-C-H stretching in between  $2917.7\text{ cm}^{-1}$  to  $2936.29\text{ cm}^{-1}$  due to the incorporated long chain of unsaturated fatty acids. The chitosan can be spotted with the existence of C=O stretching and N-H bending of amines at the peak ranges of  $1630.7\text{ cm}^{-1}$  to  $1643.86\text{ cm}^{-1}$  and  $1411.81\text{ cm}^{-1}$  to  $1529.65\text{ cm}^{-1}$ , respectively. The C-O stretching corresponds to the presence of the plasticiser, which is glycerol in the film structure along the sharp peak at  $1039.33\text{ cm}^{-1}$  to  $1070.23\text{ cm}^{-1}$ . There are also C-H bending at  $1314.83\text{ cm}^{-1}$  to  $1380.34\text{ cm}^{-1}$  and C-N stretching at  $1111.54\text{ cm}^{-1}$  to  $1151.72\text{ cm}^{-1}$ . The BSF-based chitosan films demonstrated excellent mechanical strength and barrier properties, attributed to their high crystallinity and abundance of functional groups, making them suitable for sustainable packaging applications; similar enhancements in mechanical properties have been reported in chitosan-based film from black soldier fly exuviae and reinforced with anthocyanin from red dragon fruit peel (Simon et al., 2025).



**Figure 2:** Infrared Spectra of Chitosan Films

#### 4. CONCLUSION

This study successfully demonstrated the potential of BSF spent pupal shells as a sustainable and effective source for chitosan production, with promising application for food packaging. The extraction process yielded chitosan with a high degree of deacetylation, reflecting its suitability for film formation. Physicochemical and mechanical evaluations revealed that BSF-based chitosan films possess good solubility and moderate moisture resistance, while its mechanical performance was comparatively lower than commercial chitosan films. Notably, blending BSF-chitosan with commercial chitosan at a 50:50 ratio significantly improved the tensile strength, flexibility, and barrier properties of the film. Structural characterization via FTIR and XRD confirmed the compatibility of functional groups and crystallinity essential for packaging materials. Overall, BSF-derived chitosan films present a promising, eco-friendly alternative to conventional plastic packaging. Further studies aimed at enhancing the mechanical strength of BSF-chitosan films could enhance its application in commercial food packaging production.

## ACKNOWLEDGEMENTS

The authors wish to acknowledge the Ministry of Higher Education Malaysia (MOHE) for the financial support under Grant FRGS/1/2024/TK05/UNIMAP/02/3. Appreciation is also extended to Universiti Malaysia Perlis for providing the necessary facilities and technical assistance throughout the duration of this study.

## REFERENCES

- Bhuvaneshwari, S., D, S., Velmurugan, S., Kalyani, N., & Sugunabai, J. (2011). Development and characterization of chitosan film. *International Journal of Engineering Research and Applications* (IJERA), 1(2011), 292-299.
- El Knidri, H.; Belaabed, R.; Addaou, A.; Laajeb, A.; Lahsini, A. (2018) Extraction, chemical modification and characterization of chitin and chitosan. *Int. J. Biol. Macromol.*, 120, 1181–1189. <https://doi.org/10.1016/j.ijbiomac.2018.08.139>
- Gera, R., Chadha, P., Banerjee, S. P., Sharma, M., Pandey, A. K., Kampani, S., Dixit, S., Tummala, S. K., & Gatea, M. A. (2023). A narrative review on use of biomaterials in achieving SDG 9: Build resilient infrastructure, promote sustainable industrialization and foster innovation. *E3S Web Conf.*, 391(2023), 01180-01194. <https://doi.org/10.1051/e3sconf/202339101180>
- Hahn, T., Roth, A., Ji, R., Schmitt, E., & Zibek, S. (2020). Chitosan production with larval exoskeletons derived from the insect protein production. *Journal of Biotechnology*, 310(2020), 62-67. <https://doi.org/10.1016/j.jbiotec.2019.12.015>
- Khatami, N., Guerrero, P., Martín, P., Quintela, E., Ramos, V., Saa, L., Cortajarena, A. L., de la Caba, K., Camarero-Espinosa, S., & Abarrategi, A. (2024). Valorization of biological waste from insect-based food industry: Assessment of chitin and chitosan potential. *Carbohydrate Polymers*, 324(2024), 121529-121541. <https://doi.org/10.1016/j.carbpol.2023.121529>
- Lagat, E. K., et al. (2021). "Antimicrobial Activity of Chemically and Biologically Treated Chitosan Prepared from Black Soldier Fly (*Hermetia illucens*) Pupal Shell Waste." *International Journal of Biological Macromolecules*, 183, 949–957. <https://doi.org/10.3390/microorganisms9122417>
- Liu, Y., Yuan, Y., Duan, S., Li, C., Hu, B., Liu, A., Wu, D., Cui, H., Lin, L., He, J., & Wu, W. (2020). Preparation and characterization of chitosan films with three kinds of molecular weight for food packaging. *International Journal of Biological Macromolecules*, 155(2020), 249-259. [10.1016/j.ijbiomac.2020.03.217](https://doi.org/10.1016/j.ijbiomac.2020.03.217)
- Mohan, K., Ganesan, A. R., Muralisankar, T., Jayakumar, R., Sathishkumar, P., Uthayakumar, V., Chandirasekar, R., & Revathi, N. (2020). Recent insights into the extraction, characterization, and bioactivities of chitin and chitosan from insects. *Trends in Food Science & Technology*, 105(2020), 17-42. [10.1016/j.tifs.2020.08.016](https://doi.org/10.1016/j.tifs.2020.08.016)
- No HK, Lee SH, Park NY, Meyers SP. Comparison of physicochemical, binding, and antibacterial properties of chitosans prepared without and with deproteinization process. *J Agric Food Chem.* 2003 Dec 17;51(26):7659-63. <https://doi.org/10.1021/jf030226w>
- Pedrazzani C, Righi L, Vescovi F, Maistrello L, Caligiani A, (2024). Black soldier fly as a new chitin source: Extraction, purification and molecular/structural characterization, *LWT - Food Science and Technology* 191, 115618. <https://doi.org/10.1016/j.lwt.2023.115618>

Rachtanapun, P., Klunklin, W., Jantrawut, P., Jantanasakulwong, K., Phimolsiripol, Y., Seesuriyachan, P., Leksawasdi, N., Chaiyaso, T., Ruksiriwanich, W., Phongthai, S., Sommano, S. R., Punyodom, W., Reungsang, A., & Ngo, T. M. P. (2021). Characterization of Chitosan Film Incorporated with Curcumin Extract. *Polymers*, 13(6), 963-977. <https://doi.org/10.3390/polym13060963>

Saenz-Mendoza, A. I., Zamudio-Flores, P. B., García-Anaya, M. C., Velasco, C. R., Acosta-Muñiz, C. H., de Jesús Ornelas-Paz, J., Hernández-González, M., Vargas-Torres, A., Aguilar-González, M. Á., & Salgado-Delgado, R. (2020). Characterization of insect chitosan films from *Tenebrio molitor* and *Brachystola magna* and its comparison with commercial chitosan of different molecular weights. *International Journal of Biological Macromolecules*, 160(2020), 953-963. <https://doi.org/10.1016/j.ijbiomac.2020.05.255>

Simon A., Pramitasari R., Anugrah DSB., Waturangi DE (2025) Development of intelligent packaging films utilising chitosan derived from black soldier fly exuviae and anthocyanin from red dragon fruit peel for monitoring banana ripeness. *International Journal of Biological Macromolecules*, 319 ( 3), 145610. <https://doi.org/10.1016/j.ijbiomac.2025.145610>

Soetemans L, Uyttebroek M, Bastiaens L. (2024). Characteristics of chitin extracted from black soldier fly in different life stages. *International Journal of Biological Macromolecules*, Volume 165, Part B, 15 December 2020, Pages 3206-3214 <https://doi.org/10.1016/j.ijbiomac.2020.11.041>

Ssekatawa, K., Byarugaba, D. K., Wampande, E. M., Moja, T. N., Nxumalo, E., Maaza, M., Sackey, J., Ejobi, F., & Kirabira, J. B. (2021). Isolation and characterization of chitosan from Ugandan edible mushrooms, Nile perch scales and banana weevils for biomedical applications. *Scientific Reports*, 11(1), 4116-4129. <https://doi.org/10.21203/rs.3.rs-21938/v1>

Sutharsan J, Boyer A C, Zhao J. (2022). Physicochemical properties of chitosan edible films incorporated with different classes of flavonoids. *Carbohydrate Polymer Technologies and Applications* 4 (2022) 100232. <https://doi.org/10.1016/j.carpta.2022.100232>

Yan, J., He, S., Chen, L., Chen, H., & Wang, W. (2023). Characterization, antioxidant and antibacterial activities of gelatin-chitosan edible coated films added with *Cyclocarya paliurus* flavonoids. *International Journal of Biological Macromolecules*, 253(2023), 127664-127673. <https://doi.org/10.1016/j.ijbiomac.2023.127664>

Yuan, B.Q., Yu, T.H., Chen, S.C., Zhang, Z.Q., Guo, Z.K., Huang, G.X., Xiao, J.H., & Huang, D.W. (2024). Physical and chemical characterization of chitin and chitosan extracted under different treatments from black soldier fly. *International Journal of Biological Macromolecules*, 135228. <https://doi.org/10.1016/j.ijbiomac.2024.135228>